Lawrence Berkeley National Laboratory
LBL Publications

Title
Efficiency of the Summer Monsoon in Generating Streamflow Within a Snow-Dominated Headwater Basin of the Colorado River

Permalink
https://escholarship.org/uc/item/6ck7h73j

Journal
Geophysical Research Letters, 47(23)

ISSN
0094-8276

Authors
Carroll, Rosemary WH
Gochis, David
Williams, Kenneth H

Publication Date
2020-12-16

DOI
10.1029/2020gl090856

Peer reviewed

Efficiency of the Summer Monsoon in Generating Streamflow Within a Snow-Dominated Headwater Basin of the Colorado River

Rosemary W. H. Carroll[1,2] iD, **David Gochis[3]** iD, **and Kenneth H. Williams[4,2]** iD

[1]Desert Research Institute, Reno, NV, USA, [2]Rocky Mountain Biological Lab, Gothic, CO, USA, [3]National Center for Atmospheric Research, Boulder, CO, USA, [4]Lawrence Berkeley National Laboratory, Berkeley, CA, USA

Abstract The North American Monsoon occurs July–September in the central Rocky Mountains bringing significant rainfall to Colorado River headwater basins. This rain may buffer streamflow deficiencies caused by reductions in snow accumulation. Using a data-modeling framework, we explore the importance of monsoon rain in streamflow generation over historical conditions in an alpine basin. Annually, monsoon rain contributes $18 \pm 7\%$ water inputs and generates $10 \pm 6\%$ streamflow. The bulk of rain supports evapotranspiration in lower subalpine forests. However, rains have the potential to produce appreciable streamflow at higher elevations where soil moisture storage, forest cover, and aridity are low and rebound late season streamflow $64 \pm 13\%$ from simulated reductions in spring snowpack as a function of monsoon strength. Interannual variability in monsoon efficiency to generate streamflow declines with low snowpack and high aridity, implying the ability of monsoons to replenish streamflow in a warmer future with less snow accumulation will diminish.

Plain Language Summary Monsoon rains bring much needed summer moisture to the southwestern United States, but it remains unclear whether rains have a significant effect on streamflow in the snow-dominated headwaters of the Colorado River. Lack of understanding is largely due to the difficulty in measuring rain and snowfall in steep, mountainous basins, and the effect both have on seasonal plant consumption of water. Using a hydrological model populated with ground, airborne, and synthesized climate data, we compare relative efficiency of monsoon rain to generate stream water over multiple decades in an alpine basin. Monsoon rains deliver one fifth of the basin's water and produce 10% the annual streamflow, with additions largely confined to the upper elevations of the watershed where soils are thin, water is plentiful, and forests are less abundant. In contrast, lower elevations contain dense aspen and conifer forests that consume monsoon rain and limit streamflow response. Subsequently, even strong monsoon events cannot fully replenish lost snow. Summer rains produce more streamflow during cooler years with large snow accumulation. This hints that streamflow from summer rain may diminish in a warmer future with less snow.

1. Introduction

Snowpack in mountain systems is declining worldwide with trends in snow loss expected into the future (Hock et al., 2019). Across the western United States, rising temperatures and changing precipitation patterns have decreased peak snow accumulation 15–30% since the mid-20th century (Mote et al., 2018), with the intensity and duration of these seasonal snow deficits increasing over the last 40 years (Huning & AghaKouchak, 2020). Reductions in snow cover produce a positive albedo feedback that results in higher air temperatures that promotes additional snowmelt (Hall, 2004; Ma et al., 2019). Rising temperatures can also drive larger soil evaporation and plant transpiration (evapotranspiration, ET) to reduce streamflow (Milly & Dunne, 2020). The Upper Colorado River (UCR) in the southwest United States is dependent on 90% of its flow from the snow covered headwaters of Utah, Colorado, and Wyoming (Jacobs, 2011) and is emblematic of these cascading feedbacks with 20% streamflow reductions projected by mid-21st century (Vano et al., 2012). The North American Monsoon (NAM) can bring significant rain to the region from July to September (Sheppard et al., 2002) that has the potential to buffer streamflow deficiencies related to reductions in snowpack.

The sensitivity of rainfall partitioning to ET or streamflow is a function of where a system resides on the spectrum between energy and water availability (Budyko, 1974; Orth & Seneviratne, 2013). Potential ET (PET), or the maximum amount of water transferred back to the atmosphere from the land surface if water is not limiting, is a commonly used metric to define energy availability. It varies seasonally as a function of temperature, solar radiation, vapor pressure, and wind speed (ASCE, 2005). Water availability is commonly defined by incoming precipitation (P). It is anticipated that during the summer monsoon, energy availability is greater than water availability (PET/$P > 1$), and rain is preferentially partitioned toward ET rather than streamflow. However, water availability is modified by initial soil moisture storage (Crow et al., 2018) and the lateral movement of ephemerical subsurface flow through the soil zone (interflow) (Carroll et al., 2019), both of which are influenced by snow accumulation, redistribution, and melt dynamics prior to the monsoon season. Therefore, we hypothesize that locations and climate conditions exist in the headwaters of the UCR where monsoon rains can generate appreciable streamflow. To capture complex processes dictating hydrologic stores and fluxes, we combine light detection and ranging (LiDAR) derived snow depths, precipitation, and vegetation raster maps, an observation network of weather and stream discharge, and a hydrologic numerical model of an UCR headwater basin. Using this data-model framework, we compare the efficiency of spring snow and summer rains in generating streamflow and explore first-order controls on monsoon rain efficiencies. We also examine the ability of monsoon rains to mitigate stream depletions from reduced snowfall and the importance of NAM precipitation in promoting streamflow the following year. Lastly, we extrapolate results across the UCR to provide a preliminary estimate of where and how much stream water from monsoon rain is generated.

2. Site Description and Methods

Detailed hydrologic analysis is done for the East River, Colorado (ER, 85 km^2) located within the headwaters of the UCR. Climate is continental subarctic (Peel et al., 2007). Snowmelt drives peak streamflow, typically occurring in early June and receding through the summer and fall. Observational networks related to snow and streamflow are described by others (Carroll et al., 2018; Carroll & Williams, 2019; Hubbard et al., 2018) with an overview and detailed site characterization provided in section S1. ER elevations range from 2,760 to 4,065 m with pristine alpine (26%), conifer (45%), aspen (12%), and smaller coverages by shrubs, meadows, and riparian conditions (Landfire, 2015). Two Snow Telemetry (SNOTEL) stations reside in proximity of the ER with their period of record capturing a wide range in snow accumulation and monsoon scenarios. Daily observations of solar radiation and snow depth are taken from four weather stations in the basin. Nine nested, subbasins are included in the analysis with characteristics provided in Table S1.

The ER hydrologic model tracks daily water and energy budgets at the 100-m grid resolution between the atmosphere, plant, soil, groundwater, and river subcomponents of the watershed for historical climate conditions (years 1987–2019). The model uses the US Geological Survey (USGS) Precipitation-Modeling Runoff System (PRMS; Markstrom et al., 2015). Climate forcing assigns minimum and maximum daily temperature lapse rates defined by the SNOTEL stations adjusted for aspect. PET is calculated using a modified version of the, Jensen-Haise formulation dependent on temperature and solar radiation (Jensen et al., 1969). SNOTEL snowfall is spatially distributed using LiDAR derived snow depth observations from the Airborne Snow Observatory (ASO) flown 4 April 2016 (Painter et al., 2016). Snow depths are converted to snow water equivalent (SWE) based on ground surveys and snow density modeling (Marks et al., 1999) and corrected for simulated snow water losses prior to the flight. Rainfall is spatially distributed using the 30-year average monthly Parameter-elevation Relationships on Independent Slopes Model (PRISM, 800 m) 30-year monthly averages (OSU, 2012). Model parameterization, calibration, and verification of solar radiation, snow depth, SWE, and streamflow are presented in previously published papers (Carroll et al., 2019; Fang et al., 2019) and described in sections S2 and S3.

Sensitivity of streamflow change to precipitation is simulated by removing spring (April–May) or monsoon (July–September) events for each year in the simulation independent of the other years. Water budget components are compared to the historical (baseline) condition. Regression analysis considers interannual variability in stream water response to seasonal climate and simulated internal hydrologic states and fluxes at the basin scale. Subbasin analysis considers stream water response to summer rain as a function of topographic, vegetation, and average climate metrics. The spatial analysis of ER subbasins serves as a template for
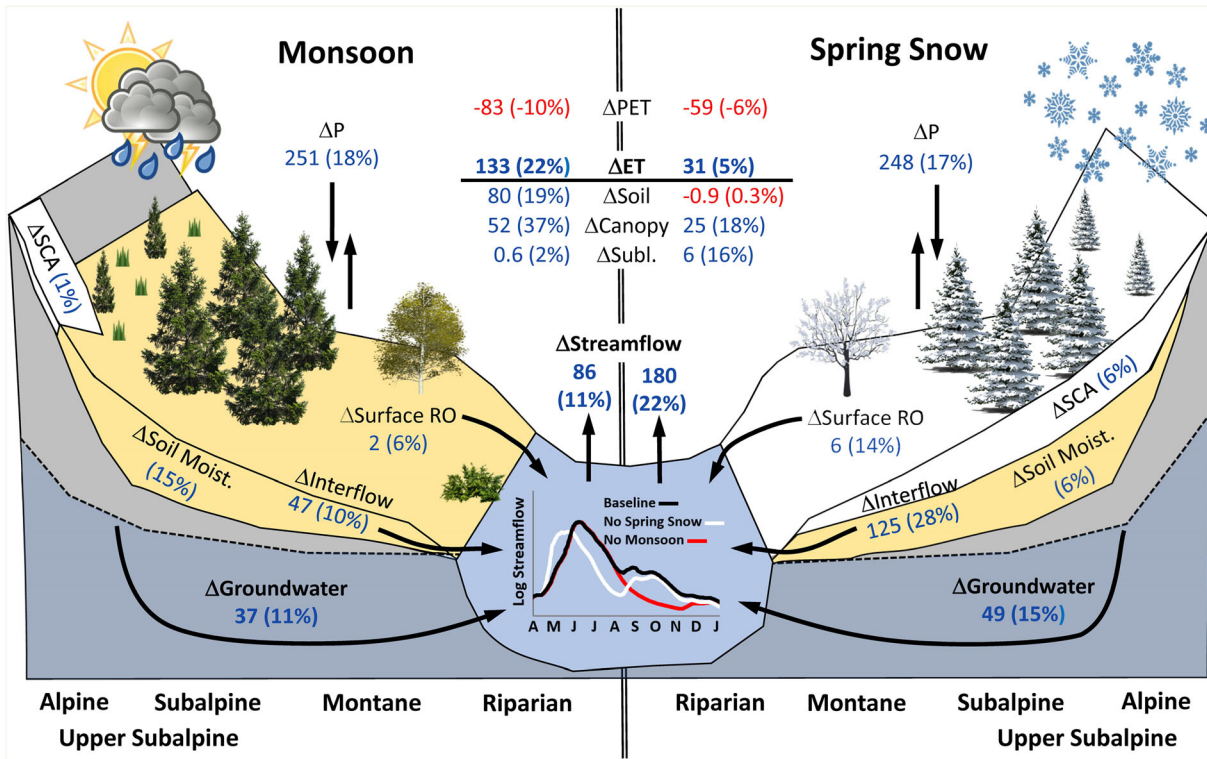
Figure 1. Average annual changes in East River simulated water stores and fluxes for monsoon (July–September) and spring (April–May) precipitation, years 1987–2019. Units are mm (% change from baseline). Blue font highlights increases and red font decreases. Δ = change; ET = evapotranspiration; P = precipitation; RO = runoff; SCA = snow covered area.

upscaling NAM streamflow generation efficiency across the UCR. Upscaling occurs at the USGS hydrologic unit code (HUC)-12 resolution (U.S. Geological Survey, 2013). Zonal statistics for topography and precipitation rely on the USGS 30-m National Elevation Dataset (U.S. Geological Survey, 2019) and PRISM monthly raster maps.

3. Results

Average annual streamflow exiting the ER is 2.16 ± 0.48 m^3/s (812 ± 204 mm/year) with flow highest in June (7.8 ± 3.4 m^3/s) and lowest in February (0.42 ± 0.19 m^3/s). Simulated precipitation is $1{,}413 \pm 233$ mm/year with $77 \pm 16\%$ falling as snow. Total annual ET for the baseline simulation is 605 ± 57 mm/year or 43% total precipitation. Estimated ET is larger than eddy covariance flux tower data located near the basin terminus (417 ± 29 mm/year) (Ryken et al., 2020), but well aligned with Niwot Ridge eddy flux tower observations in a conifer and aspen forest in Colorado (603 mm/year) (Figure S16). ET components of sublimation, canopy evaporation, and soil ET are 39 ± 6, 138 ± 19, and 428 ± 41 mm/year, respectively. A schematic of average seasonal water partitioning associated with spring snow and monsoon rain over the simulation period is given in Figure 1. Monsoon precipitation is estimated 251 ± 94 mm/year or $18 \pm 7\%$ annual water inputs. A small portion of this precipitation falls as intermittent snow at high elevations to contribute 1% to annual of snow-covered area (SCA). Cloudy conditions during storm events lower solar radiation and decrease PET. Monsoon rains increase ET (133 mm/year) largely in the soil zone in response to increased soil moisture and to a lesser degree from canopy evaporation. Monsoon rains increase streamflow by 86 mm/year or 11% annual water export. On average, spring precipitation is nearly equal to monsoon events (248 ± 94 mm) but produces twice as much streamflow (180 mm/year, 22%).

Ecozones and the spatial distribution of annual ET for year 1998 are mapped across the watershed and various energy and water budget components are collapsed to one dimension (elevation) (Figure 2). Included are the additive (positive) and reductive (negative) contributions to water budgets as a consequence
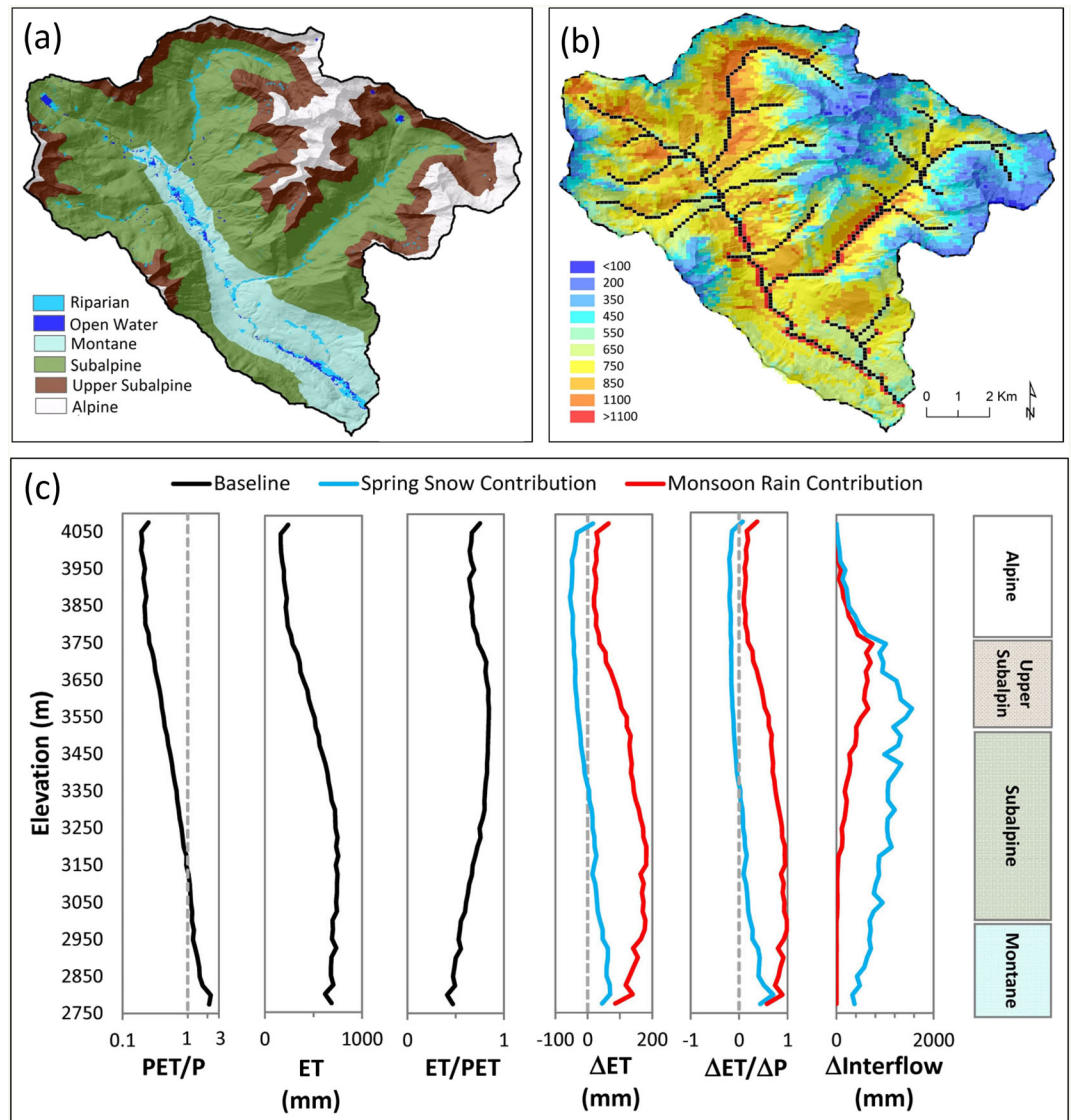
Figure 2. East River spatial patterns in (a) ecosystems and (b) 1998 evapotranspiration, ET (mm/year). (c) Elevation-averaged 1998 baseline potential evapotranspiration (PET) to precipitation (P), evapotranspiration (ET), ET/PET, ΔET, ΔET/ΔP, and Δinterflow. Change is defined as baseline minus simulation with seasonal precipitation removed.

seasonal precipitation. Year 1998 represents median snow accumulation with equal spring and summer water inputs. Alpine conditions are defined above treeline (≥3,750 m). The subalpine is defined as conifer coverage ≥50% by area (3,525–3,000 m). The upper subalpine is the transition between the alpine and subalpine containing a mix of barren and low-density conifer forests. The montane occurs at the lowest elevations and is dominated by shrubs and aspen. Annually, the ER is energy limited in upper elevations and transitions toward water limitation in the lower portions of the subalpine. ET increases with decreased elevation, and rates are at a maximum in the lower subalpine, below which rates decline slightly in response to water limitation. The ability of ET to match atmospheric demand (ET/PET) is at a maximum between 3,275 and 3,700 m. Spring snow reduces ET in the upper elevations but increases ET in the lower elevations. Interflow occurs across all elevations with the largest contributions in the upper subalpine. Water availability for ET is not fully supported by spring snow contribution at lower elevations (ΔET/ΔP < 1), implying a reliance on snowmelt-derived interflow from upslope. Monsoon events increase ET across all elevations with the largest increases in the lower subalpine. Monsoon generated interflow is largest in the upper subalpine, and no interflow occurs from rain at elevations <3,150 m. Monsoon

precipitation at lower elevations supports increases in ET (ΔET/$\Delta P \sim 1$) but at higher elevations ΔET/ΔP < 1 and increased ET relies on the down-gradient transport of storm-generated interflow to subsidize in situ rain.

Changes in daily water fluxes for 1998 are given in Figure S15. Spring snow increases SWE and SCA, and coupled with reductions in PET, snowmelt is delayed by 3 weeks. With this delay, there is an initial reduction in soil moisture that reduces ET and streamflow. However, once snowmelt begins in mid-May, ET and streamflow increase, and the net annual effect is to slightly increase total ET and promote more streamflow. ET gains are due to a net increase in sublimation and canopy evaporation in excess of a net decline in soil ET. Streamflow gains are primarily from interflow. Summer rains increase soil moisture and all ET components such that atmospheric demand is nearly satisfied following rain events (ET/PET = 1.0). Streamflow increases occur in the summer and fall.

First-order controls on ER interannual variability of monsoon precipitation and streamflow generation are explored with simple regression analysis using the Alkaike Information Criterion (AIC), coefficient of determination and statistical significance (Figure 3, details in section S4). Simulated rain anomalies in the ER oscillate over a 7- to 10-year cycle with amplitude in anomalies increasing 50% since 2013. Indirect relationships of peak SWE ($p < 0.01$) and aridity ($p < 0.01$) describe 29% of the observed variance in summer rain amounts. Across historical conditions, stream water exports are directly related to the amount of seasonal water input with summer rain half as efficient at generating streamflow compared to spring snow for the same water input. Sixty-seven percent of the simulated variance in monsoon rain efficiency (streamflow generation per unit precipitation input) is described by peak SWE ($p < 0.01$) and PET ($p < 0.01$). Simulated ET increases in response to the amount of monsoon rain, while increases in ET as a function of spring snow are much lower, and this relationship declines with larger contributing precipitation, albeit with a weak and insignificant trend ($p = 0.24$). The ability for monsoon rain to generate streamflow in the following year (lag1) is modest (3 ± 2% increase) and is predominantly driven by the size of the monsoon ($p < 0.01$), but outlier years suggest the influence of monsoon rain increases when annual conditions are cool and PET is low ($p < 0.01$). A combined nonlinear function of total rain and PET describes 70% of simulated variability ($p < 0.01$) and can explain sharp increases in subsequent year streamflow generation approaching 8%. The ability of monsoon rain to replace late season streamflow deficiencies (July–December) because of reduced spring snowfall is 64 ± 13%. Rebound in baseflow ranges from 33% to 83% and is directly related to the relative strength of monsoon inputs (R_s) defined as the ratio of monsoon rain to spring snowfall reduction ($p < 0.01$). By the end of December, monsoon rain replaces streamflow deficiencies from lost snowpack 87 ± 7% with no historical monsoon scenario obtaining 100% streamflow recovery.

Annual subbasin efficiency is described by a nonlinear, direct relationship to elevation ($r^2 = 0.94$, all terms $p < 0.01$) and by indirect relationships to forest areal coverage ($r^2 = 0.61$) and forest canopy density ($r^2 = 0.61$). Wide confidence intervals are a consequence of a small sample size (Figure 3f). The best predictive model relies only on elevation with the inclusion of forest characteristics unable to add enough additional information to improve predictive power. Extrapolation of elevation to compute monsoon rain efficiency across the UCR is provided in Figure S18. Analysis suggests only 5% of the UCR area has the potential to produce streamflow from monsoon rain. Efficiencies for these basins range from 0.3% to 42% and average 26% of monsoon inputs. Total streamflow generated is 0.84 km^3 (677,000 acre-feet). The volume of flow generated is predominantly in the state of Colorado (86%) with smaller contributions from Utah (11%) and Wyoming (3%) owing to the geographic distribution of summer rains and the elevation of headwater basins.

4. Discussion

The timing and intensity of the NAM is dominated by large-scale atmospheric processes (Zhu et al., 2005) but influences of localized land surface conditions (e.g., soil moisture) could be important. Several studies have suggested there is an inverse relationship between winter snow accumulation and summer rainfall with decreased snow accumulation driving reduced soil moisture such that less energy is needed to heat the land surface and this enhances the onset of rains (Gutzler, 2000; Lo & Clark, 2002; Zhu et al., 2005). In contrast, a positive soil moisture and rainfall feedback has been found by others (e.g., Vivoni et al., 2009), while 470 years of precipitation records reconstructed with tree ring data found the historical inverse relationship between
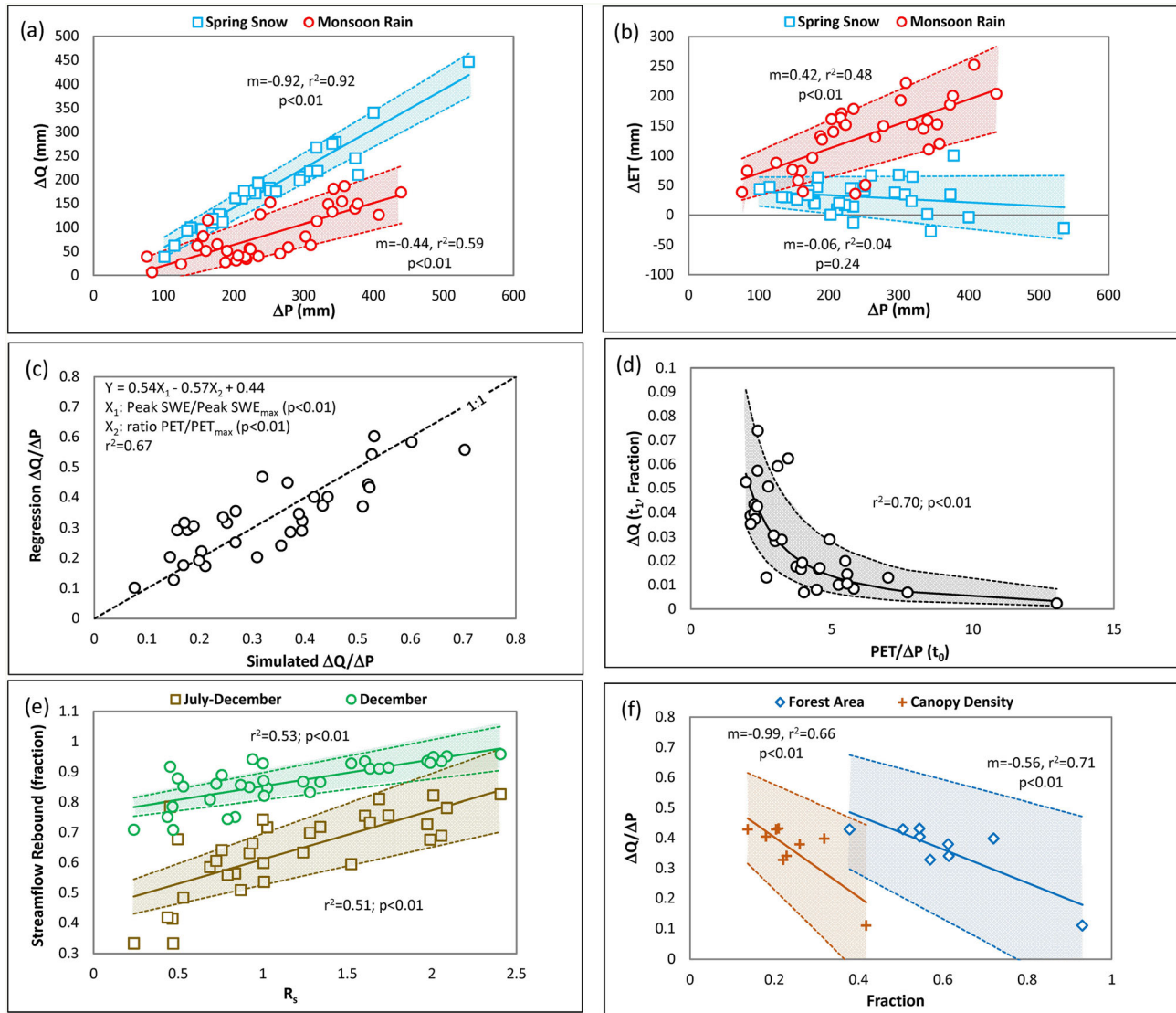
Figure 3. Annual, basin-scale water fluxes for years 1987–2019. (a) Change in streamflow (ΔQ) as a function of added precipitation (ΔP) from spring snow (April–May) or monsoon rain (July–Sept). (b) Change in evapotranspiration (ΔET) as a function of added precipitation. (c) Predictive ability of peak snow water equivalent (SWE) and potential ET (PET) to describe numerical model simulated monsoon streamflow efficiency (ΔQ/ΔP). (d) Fractional increase in streamflow (lag1, t_1) as a power function of PET and amount of monsoon rain (lag0, t_0). (d) Fraction of streamflow rebound to baseline due to lost spring snow as a function of the ratio of monsoon precipitation to reduced spring snowfall (R_s). (e) Annual average efficiency for subbasins in the East River as functions of forested area and forest canopy density. Gothic subbasin removed. Shaded areas represent the 80% confidence interval.

summer and winter precipitation weak and unstable despite appearing stronger during the latter half of the 20th century (Griffin et al., 2013). It is acknowledged the hydrologic model used in this analysis does not account for soil moisture-atmospheric feedbacks. However, the data-model integration approach indicates that ER summer rain anomalies do not correlate to premonsoon soil moisture. Instead, results show a statistically significant, indirect correlation with cumulative snow water inputs and PET. This suggests years with low snow accumulation (dry), but lower atmospheric demand (cool) might produce more summer rain, though the multiple regression's predictive power is low. Future work funded by the US Department of Energy's Atmospheric Radiation Measurement research program will, in part, focus on capturing precipitation phase, amount and intensity in the ER as well as investigate regional flow of water into the continental interior during the summer monsoon (https://www.arm.gov/news/facility/post/60749). This work will better constrain where, when, and how summer rains enter the ER.

Research presented is largely inspired by exceptionally low NAM rainfall totals experienced in the UCR in 2018 and 2019 (ER z score approx. −2) and cited by regional water managers in the UCR for reducing late season flow to unprecedented levels (Sackett, 2018) and lowering streamflow forecasts the following year (Sackett, 2020). The efficiency of seasonal precipitation to generate streamflow is related to the water availability based not only on direct water input at the land surface from rain or snowmelt but also on the subsidy of lateral interflow and the timing and location of water inputs with respect to PET and ET demand. Precipitation inputs from snowmelt are controlled by snow accumulation, redistribution, and persistence (Hammond et al., 2018; Knowles et al., 2015) with these snow dynamics highly dependent on topography, vegetation type, and stand structure (Bales et al., 2006; Tennant et al., 2017; Welch et al., 2016). For example, competing processes of canopy interception and sheltering from winds and solar radiation suggest forests with intermediate tree density promote greater snow accumulation and a later peak SWE (Broxton et al., 2015; Musselman et al., 2008). In turn, snow persistence has been found to produce more rapid snowmelt to induce soil saturation (Trujillo & Molotch, 2014), after which water can move vertically as recharge or laterally through the soil zone as interflow to promote more streamflow (Barnhard et al., 2020; Barnhart et al., 2016). Lateral movement of water is largely a function of soil storage and water holding capacity (Xiao et al., 2019) and initial soil moisture content, such that soil moisture observations can improve streamflow forecasts (Crow et al., 2018; Mahanama et al., 2012; Shahrban et al., 2018). Use of LiDAR snow observations informs where snow ends up, not necessarily where it fell. As such, the model implicitly accounts for snow redistribution by wind and avalanche as well as feedbacks between vegetation structure that may modify snow dynamics that are important to getting a more accurate depiction of where and when snowmelt enters the system, which in turn dictates if soil water can move laterally to support downgradient ET or streamflow.

Model results indicate monsoon rains in the ER generate $10 \pm 6\%$ the annual streamflow with contributions helping to sustain late season baseflow. Results fall in the reported range of streamflow generated from rain across the western US at 30% (Li et al., 2017) and 1–2% (Julander & Clayton, 2018), with the lower limit occurring in more arid climates than the ER. Years with large snow accumulation and low atmospheric water demand directly describe the efficiency of monsoon rain to generate streamflow. Under these conditions, less water is lost back to the atmosphere, and the soil moisture holding capacity is exceeded for lower amounts of water input to allow more interflow. A portion of this interflow supports downgradient ET, but some reaches the stream channel. Interflow from monsoon rain, however, is constrained to high elevations where soils are thin, forests are sparse, and ET demand is low. Lower in the landscape, premonsoon initial soil moisture content is low, and water-limiting conditions occur such that all summer rain is used to support additional ET and no interflow is generated. These lower elevations, with emphasis in the subalpine forests, effectively moderate ER streamflow response to monsoon rain through ET. From our limited subbasin sample size, the complex interplay between the amount and timing of water availability, energy demand, storage potential, and vegetation water use can be reduced to a single metric of elevation to describe spatial variability of monsoon rainfall efficiency. A simplistic extrapolation across the UCR using elevation as the determinant suggests only a 5% of the region's area has the potential to generate streamflow, but the volume generated is comparable to 15% the annual consumptive demand of the UCR (USBR, 2015), or 8% the annual UCR compact compliance to the lower basin (USBR, 1948) and is therefore significant. Future work will need to expand the data-modeling approach to enlarge the sample size and improve the statistical significance of the analysis.

The direct relationship of monsoon rain efficiency to peak SWE and indirect relationship to PET suggests a decline in monsoon-driven streamflow will occur in a future with less snow and warmer temperatures. In contrast, spring snowfall has a more complex relationship to ET in space and time driven by albedo-snowmelt feedbacks that substantively shift timing of melt and subsequent runoff (Barnett et al., 2005) but show relatively small net changes in ET compared to monsoon rains. The lower efficiency of ET to snowmelt is due to the timing of inputs prior to peak consumptive demand. This is supported by Berkelhammer et al. (2017), who found gross primary production (via satellite retrievals of solar-induced variability) in the intermountain west twice as sensitive to variations in rain compared to snow. Despite relatively low streamflow generation efficiencies in comparison to snowmelt, monsoon rain does help rebound baseflow deficiencies caused by a reduction snow accumulation. This ability is highly dependent on the relative strength of the monsoon, and no historical monsoon season can fully replenish streamflow deficits caused by hypothetical lost spring snowpack. This indicates that soil moisture dictated by snowmelt has

long lasting effects on streamflow that cannot be fully reversed with summer rain. Likewise, soil moisture memory from summer rains is hypothesized to also impose on future streamflow. McNamara et al. (2005) finds remnant dry soils in the fall remain dry once snowfall commences, and these dry soils require more meltwater than wet soils to produce lateral movement of water in the spring, thereby decreasing streamflow. Our model predicts monsoon memory on future streamflow, but the effect is modest with average annual change to future flow only to $3 \pm 2\%$. Memory is controlled by the size of the monsoon and atmospheric water demand and shows no correlation to late season soil moisture. This lack of simulated response may be due to the simplistic soil conceptualization in the hydrologic model, or it may be thin soils in headwater basins are rewetted quickly by low quantities of snowmelt in comparison to the large quantities of snow available. These relationships may change as one moves down-gradient in the UCR to warmer and drier climates, or if snow droughts continue to increase throughout the region to reduce snow accumulation in the ER. However, this requires a more detailed process-based investigation.

5. Conclusions

Summer rains are a critical water input to the ER with the amplitude of monsoon anomalies growing in the basin since 2013 and inspiring questions related to the efficiency of monsoon rains to generate streamflow. This is particularly important in the Colorado River Basin where snowpack is decreasing, and it is unknown if summer rains can buffer some of these losses. We find through a data-modeling framework that the efficiency of seasonal precipitation to produce streamflow is dictated by the timing and location of water input with respect to energy and water availability. Summer rains occur when PET is high and soil moisture is waning during the premonsoon drought. Subsequently, the bulk of rain serves to moisten very dry soils and does not generate interflow. Instead, water is quickly consumed by vegetation, with the largest increases in ET occurring in the lower subalpine dominated by aspen and conifer forests. As a result, streamflow contributions from rain are half those generated by equal amounts of spring snowfall that occur when PET is low and soils moisture is higher. Most of the rain-generated streamflow occurs at higher elevations in the watershed where soil moisture storage, forest cover, and energy demands are low. Mean elevation is the single most important predictive metric of the ability of summer rain to generate streamflow in the ER, and extrapolation estimates indicate that streamflow generation from the NAM, while limited to only 5% of the region by area, can produce substantive streamflow for either UCR consumptive demand or downstream delivery to lower basin states. Summer rain does rebound late summer streamflow from simulated reductions in snowpack as a function of monsoon strength but is unable to fully replace streamflow from lost snow accumulation even for the largest historical monsoon event. Results do show memory of monsoon rains propagate into the following year through altered baseflow but do not indicate memory as a function of fall soil moisture condition. Interannual variability in monsoon efficiency to generate streamflow declines when snowpack is low and aridity is high. This underscores the likelihood that the ability of monsoon rain to generate streamflow will decline in a warmer future with increased snow drought.

Data Availability Statement

Model characterization, validation, and additional results are provided in the Supporting Information. Model input and output files are available to the public on the US Department of Energy (DOE) Environmental Systems Science Data Infrastructure for Virtual Ecosystem (https://data.ess-dive.lbl.gov/view/doi:10.15485/1691511).

References

ASCE (2005). The ASCE standardized reference evapotranspiration equation, *Technical Committee Report to the Environmental and Water Resources Institute of the American Society of Civil Engineers from the Task Committee on Standardization of Reference Evapotranspiratio*.

Bales, R. C., Molotch, N. P., Painter, T. H., Dettinger, M. D., Rice, R., & Dozier, J. (2006). Mountain hydrology of the western United States. *Water Resources Research*, *42*, W08432. https://doi.org/10.1029/2005WR004387

Barnett, T. P., Adam, J. C., & Lettenmaier, D. P. (2005). Potential impacts of a warming climate on water availability in snow-dominated regions. *Nature*, *438*(7066), 303–309. https://doi.org/10.1038/nature04141

Barnhard, T. B., Tague, C. L., & Molotch, N. P. (2020). The counteracting effects of snowmelt rate and timing on runoff. *Water Resources Research*, *56*, e2019WR026634. https://doi.org/10.1029/2019WR026634

Barnhart, T. B., Molotch, N. P., Livneh, B., Harpold, A. A., Knowles, J. F., & Schneider, D. (2016). Snowmelt rate dictates streamflow. *Geophysical Research Letters*, *43*, 8006–8016. https://doi.org/10.1002/2016GL069690

Berkelhammer, M., Stefanescu, I. C., Joiner, J., & Anderson, L. (2017). High sensitivity of gross primary production in the Rocky Mountains to summer rain. *Geophysical Research Letters*, *44*, 3643–3652. https://doi.org/10.1002/2016GL072495

Broxton, P. D., Harpold, A. A., Biederman, J. A., Troch, P. A., Molotch, N. P., & Brooks, P. D. (2015). Quantifying the effects of vegetation structure on snow accumulation and ablation in mixed-conifer forests. *Ecohydrology*, *8*(6), 1073–1094. https://doi.org/10.1002/eco.1565

Budyko, M. I. (1974). *Climate and life*. New York: Academic Press.

Carroll, R. W. H., Bearup, L. A., Brown, W., Dong, W., Bill, M., & Willlams, K. H. (2018). Factors controlling seasonal groundwater and solute flux from snow-dominated basins. *Hydrological Processes*, *32*(14), 2187–2202. https://doi.org/10.1002/hyp.13151

Carroll, R. W. H., Deems, J. S., Niswonger, R., Schumer, R., & Williams, K. H. (2019). The importance of interflow to groundwater recharge in a snowmelt-dominated headwater basin. *Geophysical Research Letters*, *46*, 5899–5908. https://doi.org/10.1029/2019GL082447

Carroll, R. W. H., & Williams, K. H. (2019). Discharge data collected within the East River for the Lawrence Berkeley National Laboratory watershed function science focus area (water years 2015–2018). ESS-DIVE. https://doi.org/10.21952/WTR/1495380

Crow, W. T., Chen, F., Reichle, R. H., Xia, Y., & Liu, Q. (2018). Exploiting soil moisture, precipitation, and streamflow observations to evaluate soil moisture/runoff coupling in land surface models. *Geophysical Research Letters*, *45*, 4869–4878. https://doi.org/10.1029/2018GL077193

Fang, Z., Carroll, R. W. H., Schumer, R., Harman, C., Wilusz, D., & Williams, K. H. (2019). Streamflow partitioning and transit time distribution in snow-dominated basins as a function of climate. *Journal of Hydrology*, *570*, 726–738. https://doi.org/10.1016/j.jhydrol.2019.01.029

Griffin, D., Woodhouse, C. A., Meko, D. M., Stahle, D. W., Faulstich, H. L., Carrillo, C., et al. (2013). North American monsoon precipitation reconstructed from tree-ring latewood. *Geophysical Research Letters*, *40*, 954–958. https://doi.org/10.1002/grl.50184

Gutzler, D. S. (2000). Covariability of spring snowpack and summer rainfall across the Southwest United States. *Journal of Climate*, *13*(22), 4018–4027. https://doi.org/10.1175/1520-0442(2000)013<4018:COSSAS>2.0.CO;2

Hall, A. (2004). The role of surface albedo feedback in climate. *Journal of Climate*, *17*(7), 1550–1568. https://doi.org/10.1175/1520-0442(2004)017<1550:TROSAF>2.0.CO;2

Hammond, J. C., Saavedra, F. A., & Kampf, S. K. (2018). How does snow persistence relate to annual streamflow in mountain watersheds of the western U.S. with wet maritime and dry continental climates? *Water Resources Research*, *54*, 2605–2623. https://doi.org/10.1002/2017WR021899

Hock, R., Rasul, G., Adler, C., Cáceres, B., Gruber, S., Hirabayashi, Y., et al. (2019). High mountain areas. In H.-O. Portner, et al. (Eds.), *IPCC special report on the ocean and cryosphere in a changing climate* (pp. 131–202). Retrieved from https://www.ipcc.ch/srocc/chapter/chapter-2/

Hubbard, S. S., Williams, K. H., Agarwal, D., Banfield, J., Beller, H., Bouskill, N., et al. (2018). The East River, Colorado, watershed: A mountainous community testbed for improving predictive understanding of multiscale hydrological–biogeochemical dynamics. *Vadose Zone Journal*, *17*, 180061. https://doi.org/10.2136/vzj2018.03.0061

Huning, L. S., & AghaKouchak, A. (2020). Global snow drought hot spots and characteristics. *Proceedings of the National Academy of Sciences*, e201915921. https://doi.org/10.1073/pnas.1915921117

Jacobs, J. (2011). Sustainability of water resources in the Colorado River Basin. *The Bridge: Linking Engineering and Society*, *41*(winter), 6–12.

Jensen, M. E., Rob, D. C. N., & Franzoy, C. E. (1969). Scheduling irrigations using climate-crop-soil data. National Conference on Water Resources Engineering of the American Society of Civil Engineers, 20 p.

Julander, R. P., & Clayton, J. A. (2018). Determining the proportion of streamflow that is generated by cold season processes versus summer rainfall in Utah, USA. *Journal of Hydrology: Regional Studies*, *17*(December 2017), 36–46. https://doi.org/10.1016/j.ejrh.2018.04.005

Knowles, J. F., Harpold, A. A., Cowie, R., Zeliff, M., Barnard, H. R., Burns, S. P., et al. (2015). The relative contributions of alpine and subalpine ecosystems to the water balance of a mountainous, headwater catchment. *Hydrological Processes*, *29*(22), 4794–4808. https://doi.org/10.1002/hyp.10526

Landfire (2015). Existing vegetation type and cover layers. *U.S. Department of the Interior, Geological Survey*. http://landfire.cr.usgs.gov/viewer/, (accessed May 2017)

Li, D, Wrzesien, M. L., Durand, M., Adam, J., & Lettenmaier, D. P. (2017). How much runoff originates as snow in the western United States, and how will that change in the future? *Geophysical Research Letters*, 6163–6172. https://doi.org/10.1002/2017GL073551

Lo, F., & Clark, M. P. (2002). Relationships between spring snow mass and summer precipitation in the southwestern United States associated with the North American monsoon system. *Journal of Climate*, *15*(11), 1378–1385. https://doi.org/10.1175/1520-0442(2002)015%3c1378:RBSSMA%3e2.0.CO;2

Ma, J., Zhang, T., Guan, X., Hu, X., Duan, A., & Liu, J. (2019). The dominant role of snow/ice albedo feedback strengthened by black carbon in the enhanced warming over the Himalayas. *Journal of Climate*, *32*(18), 5883–5899. https://doi.org/10.1175/JCLI-D-18-0720.1

Mahanama, S., Livneh, B., Koster, R., Lettenmaier, D., & Reichle, R. (2012). Soil moisture, snow, and seasonal streamflow forecasts in the United States. *Journal of Hydrometeorology*, *13*(1), 189–203. https://doi.org/10.1175/JHM-D-11-046.1

Marks, D., Domingo, J., Susong, D., Link, T., & Green, D. (1999). A spatially distributed energy balance snowmelt model for application in mountain basins. *Hydrological Processes*, *13*(12–13), 1935–1959. https://doi.org/10.1002/(SICI)1099-1085(199909)13:12/13<1935::AID-HYP868>3.0.CO;2-C

Markstrom, S. L., Regan, R. S., Hay, L. E., Viger, R. J., Webb, R. M. T., Payn, R. A., & LaFontaine, J. H. (2015). PRMS-IV, the precipitation-runoff modeling system, version 4. In *U.S. Geological Survey Techniques and Methods, Book 6* (Chap. B7, p. 158). Reston, Virginia. https://doi.org/10.3133/tm6B7

McNamara, J. P., Chandler, D., Seyfried, M., & Achet, S. (2005). Soil moisture states, lateral flow, and streamflow generation in a semi-arid, snowmelt-driven catchment. *Hydrological Processes*, *19*(20), 4023–4038. https://doi.org/10.1002/hyp.5869

Milly, P. C. D., & Dunne, K. A. (2020). Colorado River flow dwindles as warming-driven loss of reflective snow energizes evaporation. *Science*, *9187*, 1–9.

Mote, P. W., Li, S., Lettenmaier, D. P., Xiao, M., & Engel, R. (2018). Dramatic declines in snowpack in the western US. *Npj Climate and Atmospheric Science*, *1*, 2. https://doi.org/10.1038/s41612-018-0012-1

Musselman, K. N., Molotch, N. P., & Brooks, P. D. (2008). Effects of vegetation on snow accumulation and ablation in a mid-latitude subalpine forest. *Hydrological Processes*, *22*(15), 2767–2776. https://doi.org/10.1002/hyp.7050

Orth, R., & Seneviratne, S. I. (2013). Propagation of soil moisture memory to streamflow and evapotranspiration in Europe. *Hydrology and Earth System Sciences*, *17*(10), 3895–3911. https://doi.org/10.5194/hess-17-3895-2013

OSU (2012). PRISM Climate Group. http://prism.oregonstate.edu

Painter, T. H., Berisford, D. F., Boardman, J. W., Bormann, K. J., Deems, J. S., Gehrke, F., et al. (2016). The Airborne Snow Observatory: Fusion of scanning lidar, imaging spectrometer, and physically-based modeling for mapping snow water equivalent and snow albedo. *Remote Sensing of Environment*, *184*, 139–152. https://doi.org/10.1016/j.rse.2016.06.018

Peel, M. C., Finlayson, B. L., & McMahon, T. A. (2007). Updated Koppen-Geiger climate map of the world. *Hydrology and Earth System Sciences*. https://doi.org/10.5194/hess-11-1633-2007

Ryken, A. E. C., Gochis, D., & Maxwell, R. (2020). Unraveling groundwater contributions to evapotranpiration in a mountain headwaters: Using eddy covariance to constrain water and energy fluxes in the East River Watershed. Authorea Preprints https://doi.org/10.22541/au.159559979.93668749

Sackett, H. (2018). Colorado′s 2018 water year closes out as one of the driest on record. *Aspen Times*. https://www.aspentimes.com/news/local/colorados-2018-water-year-closes-one-of-driest-on-record/

Sackett, H. (2020). Streamflow forecast down for roaring fork despite above-normal snowpack. *Aspen Times*. https://www.aspentimes.com/news/streamflow-forecast-down-for-roaring-fork-despite-above-normal-snowpack/

Shahrban, M., Walker, J. P., Wang, Q. J., & Robertson, D. E. (2018). On the importance of soil moisture in calibration of rainfall–runoff models: Two case studies. *Hydrological Sciences Journal*, *63*(9), 1292–1312. https://doi.org/10.1080/02626667.2018.1487560

Sheppard, P. R., Comrie, A. C., Packin, G. D., Angersbach, K., & Hughes, M. K. (2002). The climate of the US southwest. *Climate Research*, *21*(3), 219–238. https://doi.org/10.3354/cr021219

Tennant, C. J., Harpold, A. A., Lohse, K. A., Godsey, S. E., Crosby, B. T., Larsen, L. G., et al. (2017). Regional sensitivies of seasonal snowpack to elevation, aspect, and vegetation cover in western North America. *Water Resources Research*, *53*, 6908–6926. https://doi.org/10.1002/2016WR019374

Trujillo, E., & Molotch, N. P. (2014). Snowpack regimes of the Western United States. *Water Resources Research*, *50*, 5611–5623. https://doi.org/10.1002/2013WR014753

U.S. Geological Survey (2013). National Hydrography Dataset (NHD) for Hydrologic Unit Code (HUC)-12. https://www.usgs.gov/core-science-systems/ngp/national-hydrography/access-national-hydrography-products

U.S. Geological Survey (2019). National Elevation Dataset (NED). https://catalog.data.gov/dataset/usgs-national-elevation-dataset-ned

United States Bureau of Reclamation (2015). Provisional upper Ccolorado River Basin consumptive uses and losses report. July 2019

Upper Colorado River Basin Compact (1948). Pub. L. No. Sections 37-61-101 to 37-61–104, Colorado Revised Statutes.

Vano, J. A., Das, T., & Lettenmaier, D. P. (2012). Hydrologic sensitivities of Colorado River runoff to changes in precipitation and temperature. *Journal of Hydrometeorology*, *13*(3), 932–949. https://doi.org/10.1175/JHM-D-11-069.1

Vivoni, E. R., Tai, K., & Gochis, D. J. (2009). Effects of initial soil moisture on rainfall generation and subsequent hydrologic response during the North American monsoon. *Journal of Hydrometeorology*, *10*(3), 644–664. https://doi.org/10.1175/2008JHM1069.1

Welch, C. M., Stoy, P. C., Rains, F. A., Johnson, A. V., & Mcglynn, B. L. (2016). The impacts of mountain pine beetle disturbance on the energy balance of snow during the melt period. *Hydrological Processes*, *30*(4), 588–602. https://doi.org/10.1002/hyp.10638

Xiao, D., Shi, Y., Brantley, S. L., Forsythe, B., DiBiase, R., Davis, K., & Li, L. (2019). Streamflow generation from catchments of contrasting Lithologies: The role of soil properties, topography, and catchment size. *Water Resources Research*, *55*, 9234–9257. https://doi.org/10.1029/2018WR023736

Zhu, C., Lettenmaier, D. P., & Cavazos, T. (2005). Role of antecedent land surface conditions of north American monsoon rainfall variability. *Journal of Climate*, *18*(16), 3104–3121. https://doi.org/10.1175/JCLI3387.1